ORIGINAL PAPER

Electrical conductivity and dielectric behaviour of PPG$_4$–AgCF$_3$SO$_3$:Al$_2$O$_3$ nanocomposite gel polymer electrolyte system

S. Austin Suthanthiraraj · R. Kumar · B. Joseph Paul · Vinod Mathew

Abstract In this report, the synthesis of solvent-free poly (propylene glycol) 4000 (PPG$_4$)–silver triflate (AgCF$_3$SO$_3$): xAl$_2$O$_3$ nanocomposite gel polymer electrolytes containing four different amounts of Al$_2$O$_3$ nanoparticles corresponding to x=1, 3, 5 and 7 wt.%, respectively, with an ether oxygen-to-metal cation ratio (O–M) of 4:1 together with their vibrational spectroscopic characteristics derived from Fourier transform infrared (FT-IR) spectroscopic analysis at room temperature (25 °C) is described. Furthermore, a detailed investigation concerning their mechanism of ion transport performed by means of complex impedance analysis in the frequency range 20 Hz to 1 MHz and over the temperature region 25–90 °C and analysed in terms of electrical conductivity spectra, electrical modulus spectra and impedance spectra has indicated that the typical composition PPG$_4$–AgCF$_3$SO$_3$:5 wt.% Al$_2$O$_3$ would exhibit the best room temperature electrical conductivity of 6.2×10^{-4} S cm^{-1} owing to the mobility of coordinated silver cations through the mechanism of enhanced segmental motion of the PPG$_4$ polymer chains as aided by the various coordinating sites available within the polymer network. It is also demonstrated from the present FT-IR results that significant changes in the intensity, shape and position of the different vibrational bands corresponding to –OH stretching, C–O–C stretching, C–H stretching and C–O–C in C–H stretching modes occur as a result of the incorporation of Al$_2$O$_3$ nanofiller particles into the PPG$_4$–AgCF$_3$SO$_3$ complex. It is evident from the conductivity data that the observed enhancement in electrical conductivity would result from appropriate changes in ionic association occurring in the form of probable ion–ion and ion–polymer interactions involving Al$_2$O$_3$ nanofiller additive in accordance with the Lewis acid–base model of polymer–salt–filler interactions.

Keywords Poly(propylene glycol) · AgCF$_3$SO$_3$ · Electrical conductivity · Nanofiller

Introduction

In the realm of polymer electrolytes, systems based on poly (oxa alkanes), poly(aza alkanes), poly(thia alkanes), poly(oxa alkanes)–polyethers and alkali metal salt complexes with poly (ethylene oxide) (PEO) constitute the most intensively investigated ion-containing polymers so far owing to their particular significance for the development of polymer batteries, electrochromic windows or displays, fuel cells and electrochemical sensors. In spite of almost three decades of active research towards the design and fabrication of new polymer electrolytes, certain fundamental aspects such as low ambient temperature ionic conductivity, ionic transference numbers lower than unity and electrode/electrolyte interfacial effects appear to remain unresolved, thus offering the scope for further efforts towards improvement in their device-oriented characteristics. In this context, one of the scientifically proven and promising approaches for the realization of reduced crystallinity in the case of the chosen polymer host matrix was found to involve the synthesis of composite polymer electrolyte materials consisting of three components, namely, polymer matrix, dopant salt and a filler owing to enhanced conductivity, improved cationic transference numbers and better electrochemical stability in comparison with those unmodified polymeric systems. The area of ion-conducting composite polymeric electrolytes began with the advent of composite materials comprising commercially

S. A. Suthanthiraraj (✉) · R. Kumar · B. J. Paul · V. Mathew
Department of Energy, University of Madras—Guindy Campus, Chennai 600025, India
e-mail: suthan98@gmail.com

available microsize alumina (Al_2O_3) or silica (SiO_2) powders in conjunction with polar polymers. The recent intense interest in composite polymer electrolytes results from the widespread use of nanosized particles of conducting or non-conducting inorganic fillers in combination with a variety of polymer matrices and optimization of synthesis procedures as well. The role of the filler is essentially to alter polymer–ion and ion–ion interactions in such a manner as to effectively provide an appropriate structural framework favourable for the ionic transport [1–8].

Though the original aim to employ composite polymer electrolyte was to attain enhanced ionic conductivity in the case of PEO-based systems at ambient conditions and a number of reports are already available in literature, the most fundamental problem quite often encountered with PEO was its highly crystalline nature, thus suggesting the need for the fabrication and testing of an amorphous PEO matrix possessing appreciably high cationic conductivity in the ambient temperature range. It is now well demonstrated that significant ionic transport occurs only within the elastomeric amorphous phase of the polymer aided by the segmental motion of the polymer chains. On the other hand, the salt used should necessarily comprise of large anions and exhibit low dissociation energy in order to facilitate an effective dissociation whereas the solvent employed is expected to possess high dielectric constant, high boiling point and low melting point in addition to low viscosity [9]. From the application point of view, electrochemical sensors employing an electrode component based on polymer electrolytes would facilitate the detection of substances in poorly conducting liquids as well as in gases because of their compatibility features. Furthermore, silver ion-conducting polymer electrolyte systems containing PEO and silver triflate ($AgCF_3SO_3$) appear to be quite suitable for application areas such as membrane systems and gas sensors. As a consequence, several series of silver polymer electrolyte systems comprising PEO–silver trifluoroacetate ($AgCF_3COO$), PEO–silver tetrafluoroborate ($AgBF_4$), polyphospazene–$AgCF_3SO_3$ and poly(2-ethyl -2- oxazoline) (POX)–poly(vinylpyrrolidone) (PVP)–$AgCF_3SO_3$ (or $AgBF_4$) and poly(propylene glycol) (PPG)–$AgCF_3SO_3$ were reported in recent years [10–14].

Interestingly, previous reports on PPG of molecular weight 4,000 demonstrated its significance as a model system for the development of high molecular weight solid polymer electrolytes. Our recent investigations concerning the effect of concentration of $AgCF_3SO_3$ salt on the behaviour of ionic transport within the polymer electrolyte containing the polymer host poly(propylene glycol) of molecular weight 4,000 carried out in terms of Fourier transform infrared spectroscopic as well as electrochemical complex impedance studies further indicated the occurrence of strong interactions among the cations, anions and ether

oxygen and hydroxyl groups, thus suggesting that the coupling of segmental and structural relaxations would contribute appreciably towards the observed ionic mobility within the system [15–19]. It is also worthwhile to mention that recent advancements in the field of polymer ionics have been focused on the incorporation of a variety of nanosized ceramic fillers, such as Al_2O_3, CeO_2, ZrO_2, TiO_2, etc., into solid polymer–salt complexes based on PEO–$AgCF_3SO_3$ and polyvinylidene fluoride, PVDF–$AgCF_3SO_3$, and in almost all such systems the highest ionic conductivity has been realized only in those nano-composite polymeric electrolytes containing nanosized Al_2O_3 [20–25]. The addition of a small fraction of fumed nanosized silica fillers (∼ 5–10 % by weight) into certain low molecular weight polyethers was also reported to yield gel-type polymer electrolytes exhibiting conductivities comparable to that of liquid electrolytes incorporated into the silica matrix [26].

Encouraged by the positive effect of incorporation of nanosized inorganic fillers on the conductivity of polymer electrolytes as evidenced from the current literature and with a view to understand the exact correlation existing between the molecular structure and the conductivity mechanism in the case of a new nanocomposite polymer electrolyte system based on poly(propylene glycol) 4000, $AgCF_3SO_3$ and nanosized Al_2O_3, the present work has been undertaken. In accordance with the above-mentioned importance of research, this investigation describes the synthesis and characterization of a series of compositions of a PPG_4–$AgCF_3SO_3$–Al_2O_3 nanocomposite gel polymeric electrolyte system in terms of their vibrational spectroscopic as well as complex impedance spectroscopic properties in order to attain an insight into the ion transport behaviour of the new system under study with an ultimate aim of arriving at the influential aspects of the relevant ionic species, their mobility, ion–ion interactions and segmental motion of polymer chains present in a systematic fashion. The present work aims at design and fabrication of silver ion-based nanocomposite gel polymer electrolytes for membrane and electrochemical sensor applications at ambient conditions. The scope of vibrational spectroscopic data as an exquisite tool for probing into the structural and functional characteristics pertaining to several macromolecular systems and aggregates has prompted this work to employ Fourier transform infrared (FT-IR) analysis as an effective analytical technique [15, 27, 28]. On the other hand, the feasibility of obtaining an in-depth understanding of the mechanism of ionic conductivity occurring in a variety of polymer electrolytes by means of complex impedance analysis has motivated the present investigation based on variable-temperature impedance spectroscopy as a means of analysis of ion transport dynamics of the system chosen [29–33].

Experimental

Synthesis of nanocomposite polymer electrolytes

Commercially available chemicals of poly(propylene glycol) (MW 4000) PPG_4 (Polysciences Inc., USA), silver triflate, $AgCF_3SO_3$ (Purity > 99%, Aldrich) and Al_2O_3 nanopower (< 50 nm, Aldrich) were used as starting materials for the preparation of various compositions of the gel polymer electrolyte system PPG_4–$AgCF_3SO_3$–Al_2O_3 containing Al_2O_3 nanoparticles and by employing an ether oxygen-to-cation ratio (O–M ratio) of 4:1 for the polymer–salt host matrix during the course of the present investigation. Experimentally, four different compositions of the nanocomposite polymer gel electrolyte system PPG_4–$AgCF_3SO_3$:xAl_2O_3 corresponding to the dispersion of x wt.% Al_2O_3 (where x=1, 3, 5 and 7, respectively) were considered by taking appropriate amounts of the three constituents, viz. PPG_4, $AgCF_3SO_3$ and Al_2O_3 nanoparticles. Prior to the synthesis of these polymer electrolyte specimens, $AgCF_3SO_3$ was dried in an evacuated environment at 10^{-3} Torr on a vacuum line at 120 °C for 1 h, whereas the polymer was initially dried in a vacuum oven at 10^{-3} Torr at room temperature (25 °C) for 24 h. Subsequently, the silver salt was dissolved directly into the polymer itself at 75±5 °C followed by stringent vacuum drying of the polymer in order to facilitate the clearance of ether oxygen salts so that it would be easier for the extremely dry salt to dissociate completely into the polymeric matrix, thereby effecting a thorough solvation of the silver cations. Desired amounts of Al_2O_3 nanoparticles were separately dried in a vacuum oven at 10^{-3} Torr at 120 °C for 3 h and subsequently added into the polymer–salt complex followed by careful stirring for another 3 h. The specimens of nanocomposite gel polymer electrolyte thus obtained were vacuum-dried thoroughly and stored in a dry desiccator for further analytical studies.

Fourier transform infrared measurements

The Fourier transform infrared spectra were recorded for all the synthesized samples of the PPG_4–$AgCF_3SO_3$:xAl_2O_3 (where x=1, 3, 5 and 7 wt.%, respectively) polymer electrolyte system at room temperature on a Perkin-Elmer RX1 spectrophotometer with a wavelength resolution of 2 cm^{-1}. These measurements were carried out over a wavenumber range of 4,000 to 400 cm^{-1} by sandwiching individual specimens in between a pair of KBr pellets.

Complex impedance measurements

The temperature-dependent complex impedance data for all the synthesized specimens of the system PPG_4–$AgCF_3SO_3$:xAl_2O_3 were collected experimentally and analysed thoroughly by means of a computer-controlled Hewlett-Packard Model HP 4284A precision LCR meter over the frequency range 1 MHz–20 Hz in the temperature range 25–90 °C at an applied potential difference of 500 mV without any noticeable nonlinear effects due to the amplitude involved. The complex impedance data were obtained by employing a specially designed conductivity cell having a fixed sample thickness of 2 mm and a provision for a constant volume cylindrical cell electrode of 12-mm diameter made up of silver and teflon spacers in conjunction with another silver electrode of 10-mm diameter and suitably placed in a temperature-controlled oven during the present electrical conductivity measurements. In view of the fact that the frequency response of the sample under investigation could be represented by an equivalent circuit consisting of a parallel combination of the relevant circuit elements, namely, R and C, where R and C denote the resistance and capacitance, respectively, the resultant intercept of the semicircular impedance plot (i.e. plot of Z'' versus Z' where Z' and Z'' represent the real and imaginary parts of the complex impedance Z^*) on the real axis would indicate the bulk resistance, R_b, of the sample. All the experimentally observed impedance diagrams were best fitted with the previously mentioned equivalent circuit parameters internally by means of the Boukamp equivalent circuit software package incorporated within the system. Accordingly, the value of bulk resistance, R_b, for individual specimens at different temperatures could be evaluated accurately during the present work. The electrical conductivity (σ) was deduced from the equation

$$\sigma = 1/R_b(t/A) \tag{1}$$

where t is the thickness and A is the cross-sectional area of the specimen.

An in-depth analysis of the conductivity relaxation processes associated with the individual compositions of the chosen nanocomposite gel polymer electrolyte system PPG_4–$AgCF_3SO_3$:xAl_2O_3 was performed in terms of complex impedance and complex modulus characteristics with an ultimate objective of understanding their mechanisms of ion migration-related phenomena occurring within the present solvent-free PPG_4-based polymer complexes as a function of composition and temperature [30, 34, 35].

Results and discussion

Fourier transform infrared spectral data

Figure 1 depicts the observed Fourier transform infrared spectra in the case of four different compositions of PPG_4–

$AgCF_3SO_3$:$x$$Al_2O_3$ complexes corresponding to x=1, 3, 5 and 7 wt.%, respectively, indicating interesting structural features associated with various ionic interactions and complexation within these poly(propylene glycol)–silver triflate-based electrolyte specimens. It is well known that, in the case of a polymer–salt complex, the free ions are more likely to be formed as a result of dissociation of the salt wherein the cation–anion interaction is relatively weak and that the solvation of a salt in poly(propylene glycol) involved the coordination of the cation to the ether oxygens and OH terminal groups of the polymer network itself. Remarkably, the appearance of the characteristic band at ~1,032 cm^{-1} in the FTIR spectra observed for the four different compositions containing 1, 3, 5 and 7 wt.% Al_2O_3 as shown in Fig. 1 tends to suggest the complexation between PPG_4 and $AgCF_3SO_3$ and the above band may be assigned to the symmetric SO_3 mode of vibration of free triflate ($CF_3SO_3^-$) ion resulting from the probable dissociation of the silver salt and the apparently weak ion pairing between the silver cations and triflate anions [17]. A careful examination of Fig. 1 reveals that significant changes in the intensity, shape and position of the various vibrational bands corresponding to –OH stretching, C–O–C stretching, C–H stretching and C–O–C in C–H stretching modes are evident as a result of the incorporation of Al_2O_3 nanofiller particles into the PPG_4–$AgCF_3SO_3$ complex as compared to that of the uncomplexed host polymer matrix [36]. The fact that the symmetric C–O–C stretching mode appears at ~1,107 cm^{-1} in all the four different compositions of the PPG_4–$AgCF_3SO_3$:x Al_2O_3 nanocomposite gel polymer electrolyte system (where x=1, 3, 5 and 7 wt.%, respectively) instead of the typical wavenumber of 1,110 cm^{-1} tends to clearly indicate the strength of interactions existing between silver cations, ether oxygen and the –OH end groups. In addition, the observed structural features of poly(propylene glycol) in terms of –OH stretching, C–O–C stretching, C–H stretching and symmetric SO_3 modes may be ascribed to those bands noticed at ~3,160–3,140, ~1,110–1,107, ~1,357 and ~630 cm^{-1}, respectively, as in the case of previous reports on the poly(propylene glycol)–lithium triflate and poly(propylene glycol)–silver triflate-based polymer complexes [13, 19]. On the other hand, the appearance of an absorption band at ~894 cm^{-1} in the case of the specimen having 1 wt.% Al_2O_3 and its reduced intensity in the case of the sample containing 5 wt.% Al_2O_3 tend to suggest that the process of Ag^+–$CF_3SO_3^-$ ion pair formation is affected by the incorporation of Al_2O_3 nanoparticles into the PPG_4–$AgCF_3SO_3$ matrix and that the most favourable composition would correspond to the typical specimen with 5 wt.% Al_2O_3 owing to the release of the maximum concentration of free $CF_3SO_3^-$ ions. In other words, the free ion concentration is found to increase with increasing Al_2O_3 content from 1 to 5 wt.% and

becomes saturated beyond such an optimum concentration in view of the fact that, in the case of a higher concentration of 7 wt.% Al_2O_3, the formation of Ag^+–$CF_3SO_3^-$ ion pairs is quite evident from the strong band around 894 cm^{-1} as seen in Fig. 1. It is interesting to notice from Fig. 1 that the terminal –OH group also plays an important role in the dissociation of the silver salt, resulting in significant changes in –OH stretching owing to the –OH stretching vibrational modes noticed at ~3,160–3,140 cm^{-1} in the case of poly(propylene glycol) hydrogen bonded to the $CF_3SO_3^-$ anions and the oxygen bonded to the silver cation. Furthermore, the appearance of an asymmetric SO_3 stretching mode at ~1,267 cm^{-1} in the case of all the four different compositions of the present system PPG_4–$AgCF_3SO_3$: $x$$Al_2O_3$ (where x=1, 3, 5 and 7 wt.%, respectively) which is slightly lower than the characteristic vibrational frequency of 1,272 cm^{-1} corresponding to the asymmetric SO_3 mode of $AgCF_3SO_3$ salt tends to reveal that the asymmetric SO_3 stretching mode is highly sensitive to changes in the coordination state of the anion and that anions are relatively free in all the Al_2O_3 nanofiller-dispersed compositions of the chosen gel polymeric system. The above feature may be assigned to the increase in free anions due to the presence of strong interactions of the ether oxygen–silver and weak interactions between cations and anions within the polymer complex [37, 38]. It may be clearly seen from Fig. 2 that
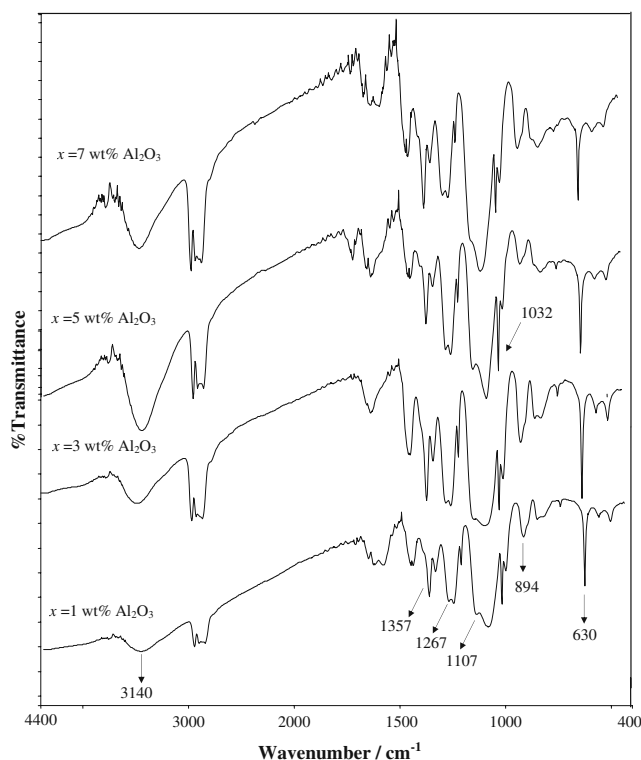

Fig. 1 FT-IR spectra of PPG_4–$AgCF_3SO_3$:$x$$Al_2O_3$ complexes with varying concentration of Al_2O_3 nanoparticles

Fig. 2 Characteristic SO$_3$ stretching mode of PPG$_4$–AgCF$_3$SO$_3$: xAl$_2$O$_3$ complexes (where x=1, 3, 5 and 7 wt.%, respectively)

the intensity of the shoulder peak at 1,032 cm^{-1} increases with increasing concentration of Al$_2$O$_3$ nanofiller up to 5 wt.% and the maximum intensity is observed for the sample having 5 wt.% nanofiller whereas a reduction in intensity is noticed in the case of the filler concentration of 7 wt.% Al$_2$O$_3$. This characteristic feature of increasing intensity of the shoulder peak appears to occur as a result of enhanced free anion concentration.

From the above discussion, it is reasonable to infer that the typical composition PPG$_4$–AgCF$_3$SO$_3$:5 wt.% Al$_2$O$_3$ may probably be associated with the presence of the maximum number of free cations and anions within the polymer matrix and hence expected to exhibit interesting ion transport properties, too.

Electrical conductivity data analysis

Figure 3 presents the complex impedance diagrams, i.e. Nyquist plots obtained for the nanocomposite gel polymer electrolyte system PPG$_4$–AgCF$_3$SO$_3$:xAl$_2$O$_3$ (where x=1, 3, 5 and 7 wt.% respectively) at room temperature (25 °C), indicating the effect of composition and ion–polymer interactions on their shapes [31]. It is clear from Fig. 3 that the intercept on the real (Z') axis representing the bulk resistance (R_b) of the specimen decreases as the concentration of Al$_2$O$_3$ nanoparticles is increased from 1 to 5 wt.% and increases further with an additional incorporation of Al$_2$O$_3$ to a higher value of 7 wt.%. As a consequence, the electrical conductivity is expected to exhibit an increasing behaviour due to the incorporation of Al$_2$O$_3$ nanofillers over the composition range from 1 to 5 wt.%, whereas a reverse trend is anticipated beyond the optimum concentration of 5 wt.%. Interestingly, the room temperature electrical conductivity (σ $_{25}$ °C) data determined for the four different compositions of the nanocomposite gel polymer electrolyte

PPG$_4$–AgCF$_3$SO$_3$:xAl$_2$O$_3$ corresponding to x=1, 3, 5 and 7 wt.% were found to be 2.7×10^{-4}, 3.4×10^{-4}, 6.2×10^{-4} and 1.3×10^{-4} S cm^{-1}, respectively. It is therefore evident that the increase in conductivity is related to the concentration region in which a high degree of ionic association is expected to occur. The enhancement in conductivity is therefore presumed to result from appropriate changes in ionic association owing to probable ion–ion and ion–polymer interactions involving the inorganic additive namely Al$_2$O$_3$ nanofiller, thus leading to changes in the fraction of ionic associates coupled with the lowering of the electrolyte viscosity in accordance with the Lewis acid–base model of the polymer–salt–filler interactions [39]. Essentially, the observed electrical conductivity of these nanocomposite polymer electrolytes would depend upon the equilibrium of the Lewis acid–base reactions involving the chosen additive, the polymer matrix and the dopant salt with anions serving as Lewis bases and cations acting as Lewis acids as reported earlier in a number of polymeric electrolyte systems based on high and low molecular weight polymer matrices [40]. The surfaces of the filler particles seem to act as cross-linking centres for the host polymer and the dopant salt, thus modifying the structure which may result in the creation of conduction pathways for ionic migration within the network. The fact that the maximum electrical conductivity at room temperature has been noticed in the case of the typical composition, PPG$_4$–AgCF$_3$SO$_3$:5 wt.% Al$_2$O$_3$ appears to reveal that the conduction mechanism is highly dependent on the Lewis acid–base interactions occurring between the surfaces of the Al$_2$O$_3$ nanofiller particles, silver cations, triflate anions and the host polymer base groups in terms of the promotion of
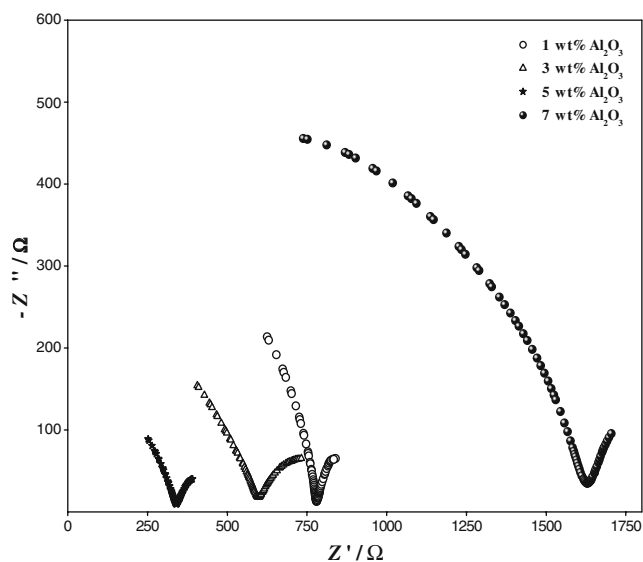

Fig. 3 Complex impedance diagrams of PPG$_4$–AgCF$_3$SO$_3$:xAl$_2$O$_3$ complexes having four different concentrations, viz. 1, 3, 5 and 7 wt.% Al$_2$O$_3$ nanoparticles at room temperature (25 °C)

dissociation of the silver salt, namely, $AgCF_3SO_3$ and lowering of ion–ion pair products, thus resulting in an enhanced ion transport within the structural framework of the above specimen. Interestingly, a decrease in the conductivity value noticed beyond the incorporation of 5 wt.% Al_2O_3 nanofiller may be most likely to be associated with the formation of certain discontinuous phases or non-conducting particle aggregates, thus resulting in a less favourable environment for ionic conduction processes. It is therefore obvious that the best conducting composition would be the typical PPG_4–$AgCF_3SO_3$–Al_2O_3 sample having 5 wt.% Al_2O_3 nanoparticles possessing the conductivity of 6.2×10^{-4} S cm^{-1} at 25 °C in good agreement with structural features revealed through vibrational spectroscopic results as discussed earlier. The segmental chain motion and percolation between ether oxygen sites would primarily govern the transport of the silver cation either strongly coordinated to –OH end groups or more weakly bound to the ether oxygen of the polymer chain. The enhanced Ag^+ ionic conductivity associated with the precise polymer–salt–filler composition containing 5 wt.% Al_2O_3 nanoparticles may be attributed to an increase in the number of mobile charge carriers, viz. monovalent silver ions. As a consequence, the free anions appear to provide additional sites, resulting in a significant increase in the mobility of the cation as well as the percolation process for an enhanced polymer segmental motion, too.

Figure 4 shows the complex impedance plots, i.e. Nyquist plots obtained for the nanocomposite gel polymer electrolyte sample PPG_4–$AgCF_3SO_3$:5 wt.% Al_2O_3 at eight different temperatures, viz. 25, 30, 40, 50, 60, 70, 80 and 90 °C, respectively. It is interesting to notice from Fig. 4 that all these Nyquist plots consist of semicircular arcs at
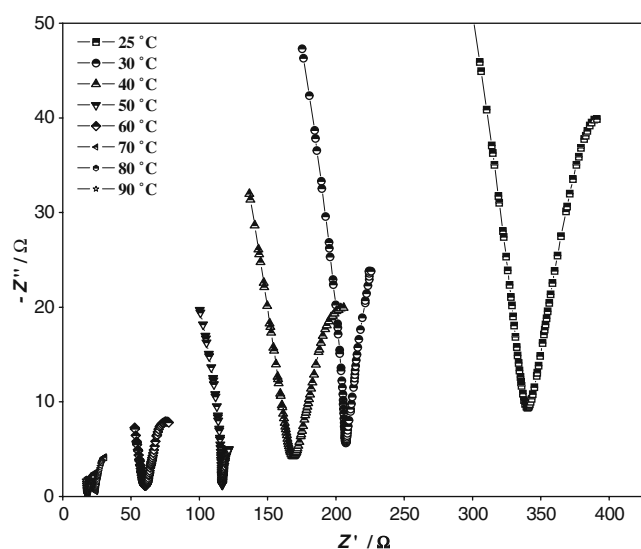
Fig. 4 Complex impedance diagrams obtained for the PPG_4–$AgCF_3SO_3$:5 wt.% Al_2O_3 sample at eight different temperatures

high frequencies which are attributed to the bulk properties of the material and low-frequency spikes owing to diffusion-controlled Warburg impedances. The appearance of a single semicircle is indicative of a geometrical capacitance and a bulk resistance connected in parallel with each other. It is also found that the point of intersection on the real (Z') axis is shifted towards the high-frequency region with increase in temperature, thus indicating the ionic transport phenomenon. These features may be explained on the basis of ion transport mechanism occurring through the various coordinating sites, local structural relaxation processes and segmental motion of the polymer chain. Accordingly, the mobility of the polymer chain is enhanced at elevated temperatures thus resulting in an increased fraction of free volume within the polymer electrolyte. In other words, the observed conductivity enhancement of the PPG_4–$AgCF_3SO_3$–Al_2O_3 polymer gel electrolyte may be attributed to the consequence of the percolation effect resulting in a considerable increase in the segmental motion of the polymer chain and hence an enhanced Ag^+ ionic conduction [19, 30]. Furthermore, the dependence of the electrical conductivity (σ) of PPG_4–$AgCF_3SO_3$:$x$$Al_2O_3$ polymer complexes where $x=1, 3, 5$ and 7 wt.% on the reciprocal absolute temperature over the region 25–90 °C is represented in Fig. 5. As expected, Fig. 5 suggests that all the observed Arrhenius plots of electrical conductivity of the chosen composition of the nanocomposite gel polymer electrolyte system PPG_4–$AgCF_3SO_3$–Al_2O_3 exhibit linear dependence which may be attributed to the fact that the ionic mobility of the charge carriers, namely, Ag^+ ions, increases with an increase in free volume of the composite polymer electrolyte system. From the linear fits of these Arrhenius plots, the values of activation energy for ionic transport for the four different compositions of the nanocomposite polymer electrolyte system corresponding to $x=1, 3, 5$ and 7 wt.% Al_2O_3 were estimated to be 0.4, 0.39, 0.37 and 0.44 eV, respectively. The fact that these activation energies are comparable to that of PPG_4–$AgCF_3SO_3$ tends to reveal the excellent complexation between PPG_4–$AgCF_3SO_3$ and Al_2O_3 nanofiller materials during the present investigation.

Figure 6 depicts the plots of frequency-dependent electrical conductivity observed at room temperature (25 °C) for the four different compositions of the nanocomposite polymer electrolyte system PPG_4–$AgCF_3SO_3$:$x$$Al_2O_3$ where $x=1, 3, 5$ and 7 wt.%, respectively, in the frequency domain 20 Hz–1 MHz. It is clear from Fig. 6 that each conductivity spectrum is characterized by the appearance of a less frequency-dependent region in the low-frequency domain which may be ascribed to the electrode polarization effects. On the other hand, the frequency-independent plateau region is seen in the mid-frequency region which, when extrapolated to the zero frequency, would correspond to the dc
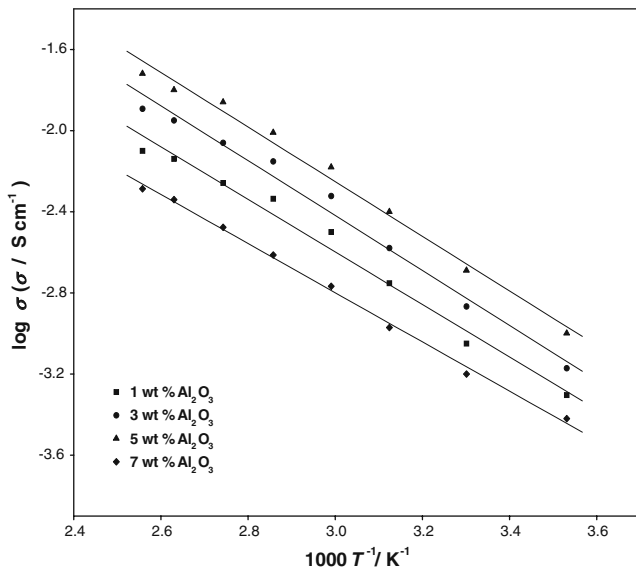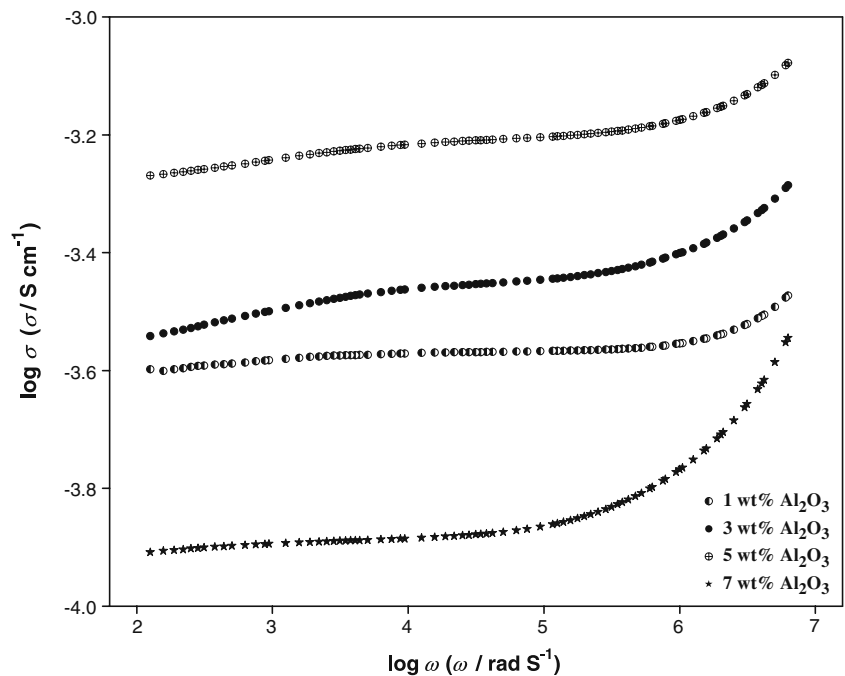
Fig. 5 Temperature-dependent electrical conductivity (σ) plots of PPG$_4$–AgCF$_3$SO$_3$:x wt.% Al$_2$O$_3$ polymer complexes with varying concentrations of Al$_2$O$_3$ nanoparticles (where $x=1$, 3, 5 and 7 wt.%, respectively)

conductivity of the sample. A closer inspection of the conductivity spectra shown in Fig. 6 appears to suggest that the highly frequency-dependent region of these spectra over the high-frequency region would indicate both forward and backward displacements of the mobile ions under the influential application of the ac signal frequency, thus exhibiting bulk characteristics of the material. As expected, it is also obvious from Fig. 6 that the electrical conductivity is maximum in the case of the

typical composition PPG$_4$–AgCF$_3$SO$_3$:5 wt.% Al$_2$O$_3$ over the entire range of frequency chosen under this study, probably due to the presence of favourable conduction pathways for Ag$^+$ ionic migration aided through the segmental motion of polymer chains [40].

The observed variations of electrical conductivity of the best conducting composition of the nanocomposite gel polymer electrolyte system PPG$_4$–AgCF$_3$SO$_3$–Al$_2$O$_3$ having 5 wt.% Al$_2$O$_3$ nanoparticles at seven different temperatures, viz. 30, 40, 50, 60, 70, 80 and 90 °C, as a function of frequency are presented in Fig. 7. It is interesting to note from Fig. 7 that each isotherm is characterized by three distinct regions, namely, the low frequency spike, the mid-frequency plateau and the high frequency spike as in the case of other polymer electrolytes [30]. The observed steep increase in conductivity (σ) at high frequencies may be attributed to correlated ionic motions within the polymer electrolyte bulk specimen. In order to characterize the ac electrical response in terms of non-linear least squares technique and impedance data, an in-depth analysis was performed by fitting the estimated σ (ω) data in the high-frequency and mid-frequency regions with the Jonscher's universal power law equation [41]

$$\sigma(\omega) = \sigma_o(\omega) + A\omega^s \qquad (2)$$

where σ_o (ω) is the dc conductivity, A is the temperature-dependent parameter and S is the fractional exponent value lying between 0 and 1. Curves obtained by fitting the impedance data using non-linear least squares technique are denoted by continuous lines in Fig. 7 and appear to reveal that there is a good agreement between the Jonscher's

Fig. 6 Electrical conductivity spectra obtained for PPG$_4$–AgCF$_3$SO$_3$:xAl$_2$O$_3$ complexes at 25 °C (where $x=1$, 3, 5 and 7 wt.%, respectively)

Fig. 7 Temperature-dependent conductivity spectra of the best conducting composition PPG$_4$ – AgCF$_3$SO$_3$:5 wt.% Al$_2$O$_3$
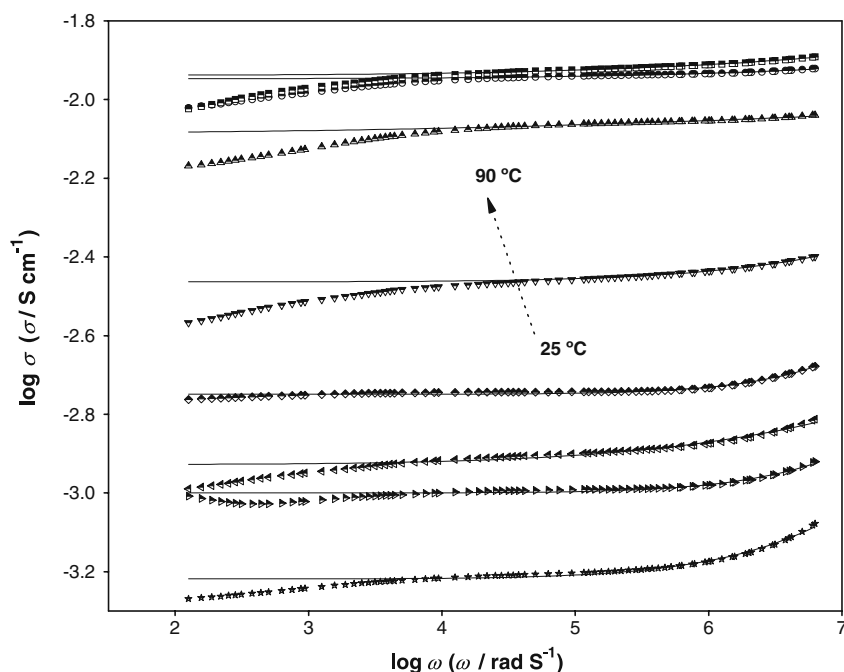
universal power law and the observed behaviour of frequency-dependent electrical conductivity of the present nanocomposite gel polymer electrolyte system at various temperatures as reported earlier in the case of several disordered inorganic solid electrolyte materials [42]. Furthermore, the value of S was found to decrease as the temperature was increased from 30 to 80 °C. This behaviour appears to suggest that the high-frequency dispersion present in the polymer electrolyte material may be attributed to many body effects arising due to ion–ion interactions within the polymer matrix and hence a non-Debye type of dielectric relaxation phenomena [43]. The observed non-Debye type behaviour of dielectric relaxation may be explained by assuming a distribution of relaxation times (DRT) arising probably due to the presence of composites of highly mobile polymer chains, silver cations and triflate anions involved in hydrogen-bonding cages with end OH groups of polymer chains and distributed as free anions within the polymer network. The overall conductivity mechanism may involve the ionic correlation process between the cations and anions distributed in the bulk material and reorganization process occurring as a result of hopping of dipoles within the coordination cage structures [30].

It is quite evident from the above discussion that the nanocomposite polymer electrolyte system PPG$_4$–AgCF$_3$SO$_3$–Al$_2$O$_3$ has indicated the occurrence of a competition between the Lewis acid site of cation and the Lewis acid centres of the nanofiller to react with the polymer base centres. In view of the fact that PPG has the Lewis base site of ether oxygen while silver triflate

(AgCF$_3$SO$_3$) contains the monovalent silver cation, which is a strong Lewis acid, as well as the large anion, CF$_3$SO$_3^-$, which constitutes the Lewis base, there exists a probability of various acid–base reactions occurring within the system. The concentration dependence of such a Lewis acid–base mechanism in terms of the filler nanoparticles incorporated into the polymer matrix may be explained on the basis of the ease with which the presence of very low nanofiller content favours the probability of interactions between the acid sites of filler particles and the base centres of the polyether chain, thus providing an increase in the cation acid sites.

On the other hand, at higher concentrations of the nanofiller, for instance 7 wt.% Al$_2$O$_3$, there is a likelihood of enhanced cross-linking centres being formed, thereby preventing the segmental motion of the polymer chains and resulting in decreased ion transport processes due to the corresponding reduction in the ion transport pathway. It is therefore most probable that 5 wt.% Al$_2$O$_3$ would correspond to the threshold concentration at which all the appropriate Lewis acid–base interactions would favourably overlap and loosen the bond strength between cations and anions, thus leading to an appreciable increase in the concentration of the mobile cation, namely, Ag$^+$ ion. Beyond this threshold concentration, e.g. 7 wt.% Al$_2$O$_3$, the formation of non-conducting (ion pairs and aggregates) sites may be responsible for a less favourable environment for the fast ion conduction process to occur. Incidentally, the formation of ion–ceramic interactions occurring in the case of low concentrations of Al$_2$O$_3$ would have resulted in a decrease in viscosity of the electrolyte associated with the

corresponding increase in the polymer chain flexibility, thus accounting for enhancing the conductivity as confirmed by the observed changes in the position of the vibration band of C–O–C stretching mode during the present FT-IR analysis as well.

Furthermore, in the context of dissociation of the silver salt, viz. $AgCF_3SO_3$, into the PPG polymer matrix, the coordination sites of Ag^+ ions appear to play a crucial role in determining the structural modifications and transport characteristics within the polymer–salt complex. Our recent reports on PPG–$AgCF_3SO_3$ complexes involving O–M ratios in the region 2:1 to 6:1 indicated the concentration dependence of effective interactions between the silver cation and ether oxygen occurring due to possible cross-linking and dilution effects [17, 18]. Accordingly, during the present investigation, the exact coordination of the silver cation with the ether oxygen corresponding to an O–M ratio of 4:1 may be treated as four owing to the increase in the inter-chain distance between the silver cation and ether oxygen within the various specimens chosen.

Modulus and impedance spectral data analysis

In order to investigate the correlation between the structural features and the conductivity mechanism and to understand the influence of the coordination sites and ionic species present within the bulk materials on the observed conductivity of the nanocomposite polymer electrolytes, a combined analysis involving conductivity and modulus spectral formalisms on the basis of the present impedance spectroscopic data has been followed. The normalized modulus spectra obtained in the form of plots of M''/M''_{max} versus $\log\omega$ where M'' denotes the imaginary part of modulus and ω is the angular frequency at eight temperatures, namely, 25, 30, 40, 50, 60, 70, 80 and 90 °C, for the best conducting complex PPG$_4$–$AgCF_3SO_3$:5 wt.% Al_2O_3 are presented in Fig. 8. From Fig. 8, it is interesting to note that all the plots exhibit a similar shape with a long and flat tail extending from the low frequency region up to the intermediate frequency region. This type of behaviour may be ascribed to the large capacitance associated with the electrodes and the observed peaking curve at high frequencies may be due to the bulk effect [44]. The non-perturbed shape of the modulus spectra at various temperatures strongly indicates the occurrence of non-Debye type of relaxation and a DRT which is almost temperature independent as in the case of PPG$_4$–$AgCF_3SO_3$ complexes [18]. The fact that all the present modulus spectra are superimposable tends to clearly reveal the feasibility of an enhancement of localized segmental motion of the mobile charge species at higher frequencies as evidenced from the presence of the conductivity relaxation mechanism which is found to be almost independent of temperature.
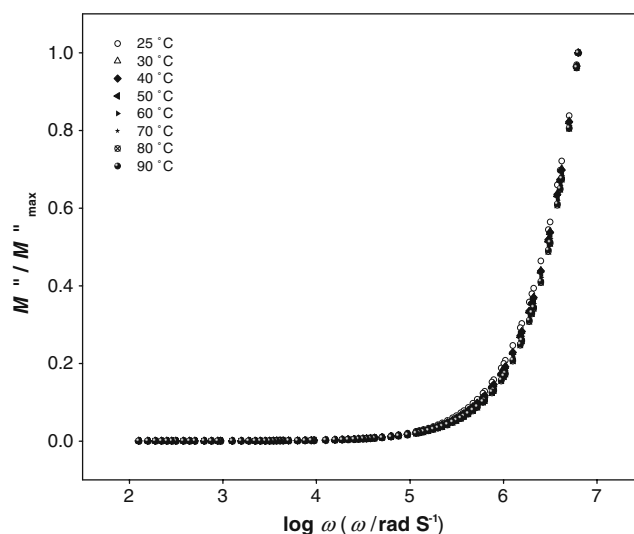

Fig. 8 Normalized modulus spectra obtained for the composition PPG$_4$–$AgCF_3SO_3$:5 wt.% Al_2O_3 as a function of temperature

The normalized impedance spectra obtained for the complex PPG$_4$–$AgCF_3SO_3$:5 wt.% Al_2O_3 at eight different temperatures, 25, 30, 40, 50, 60, 70, 80 and 90 °C, respectively, are depicted in Fig. 9. In Fig. 9, the observed low-frequency peaks may be attributed to the electrode/electrolyte interfacial effects, whereas the high-frequency peaking pattern may be assigned to the bulk relaxation occurring in these polymer composite materials. A comparison between the above sets of modulus and impedance spectra appears to suggest that the segmental motion of the polymer chain along with silver cation or the displacement of silver cation from one site to another within the composite polymer electrolyte would result in a very low relaxation time, thus implying a fast ionic migration of the cation. On the other hand, the displacement of ions at
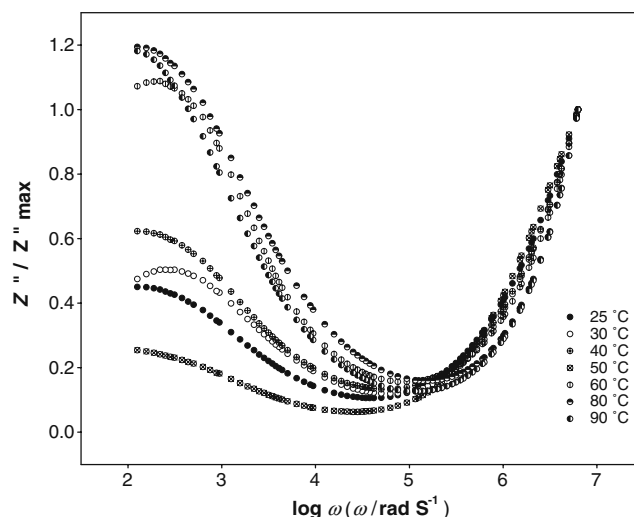

Fig. 9 Normalized impedance spectra obtained for the composition PPG$_4$–$AgCF_3SO_3$:5 wt.% Al_2O_3 as a function of temperature

higher frequencies may be coupled effectively with simultaneous backward and forward hopping phenomena resulting in a relaxation of dipoles which is expected to be less temperature dependent.

Conclusions

Electrical spectroscopic investigations involving electrical conductivity, modulus and impedance spectra carried out on a series of compositions of the nanocomposite gel polymer electrolyte system PPG_4–$AgCF_3SO_3$–Al_2O_3 containing Al_2O_3 nanofiller additive, in conjunction with a detailed structural analysis based on their vibrational spectroscopic data, have strongly indicated that the composition, temperature and nature of ion–ion and ion–polymer interactions influence the electrical conductivity mechanism and related characteristics. The appreciably high-room-temperature (25 °C) electrical conductivity of the order of 10^{-4} S cm^{-1} realized in the case of the composition having 5 wt.% Al_2O_3 nanoparticles could be attributed to the enhanced mobility of coordinated silver cations involving coordinating sites, local structural relaxation and segmental motion of the polymer chain.

References

1. Gray FM (1991) Solid polymer electrolytes: fundamentals and technological applications. VCH, New York
2. Bruce PG (1995) Solid state electrochemistry. Cambridge University Press, Cambridge
3. Croce F, Persi L, Scrosati B, Fiory FS, Plichta E, Hendrickson MA (2001) Electrochim Acta 46:2457
4. Wieczorek W, Siekierski M (2008) In: Knauth P, Schoonman J (eds) Nanocomposites—ionic conducting materials and structural spectroscopies. Springer, New York, p 1
5. Croce F, Appetecchi GB, Persi L, Scrosati B (1998) Nature 394:456
6. Bhattacharya AJ, Maier J (2004) Adv Mater 16:811
7. Osawa T, Kono M (2009) In: Yoshio M, Brodd RJ, Kozawa A (eds) Lithium-ion batteries. Springer, New York, p 413
8. Huggins RA (2009) Advanced batteries: materials science aspects. Springer, New York
9. Schantz S (1991) J Chem Phys 94:6296
10. Yoon Y, Won J, Kang YS (2000) Macromolecules 33:3185
11. Eliasson H, Albinsson I, Mellander BE (1998) Electrochim Acta 43:1459
12. Sunderrajan S, Freeman BD, Hall CK, Pinnau I (2001) J Membrane Sci 182:1
13. Eliasson H, Albinsson I, Mellander BE (2000) Mater Res Bull 35:1053
14. Jin JH, Hong SUK, Won J, Kang YS (2000) Macromolecules 33:4932
15. Kim JH, Min BR, Kim CK, Won J, Kang YS (2002) J Phys Chem B 106:2786
16. Ferry A, Oradd G, Jacobsson P (1997) Macromolecules 30:7329
17. Suthanthiraraj SA, Kumar R, Paul BJ (2009) Spectrochim Acta: A 71:2012
18. Suthanthiraraj SA, Kumar R, Paul BJ (2010) J Appl Electrochem 40:401
19. Suthanthiraraj SA, Kumar R, Paul BJ (2010) Ionics 16:145
20. Scrosati B, Croce F, Panero S (2001) J Power Sources 100:93
21. Dissanayake MAKL, Jayathilaka PARD, Bokalawela RSP (2005) Electrochim Acta 50:5602
22. Croce F, Curini R, Martinelli A, Persi L, Ronci F, Scrosati B (1999) J Phys Chem B 103:10632
23. Michael MS, Jacob MME, Prabaharan SRS, Radhakrishna S (1997) Solid State Ionics 98:167
24. Suthanthiraraj SA, Sheeba DJ (2007) Ionics 13:447
25. Suthanthiraraj SA, Paul BJ (2007) Ionics 13:368
26. Zhou H, Fedkiw PS (2004) Solid State Ion 166:275
27. Burba CM, Frech R, Grady B (2007) Macromolecules 33:3185
28. Ferry A, Jacobsson P, Torell LM (1995) Electrochim Acta 40:2369
29. Noto VD (2000) J Phys Chem 104:10116
30. Noto VD, Vittadello M, Lavina S, Fauri M, Biscazzo S (2001) J Phys Chem B 105:4584
31. Noto VD (2002) J Phys Chem B 106:11139
32. Noto VD, Vittadello M, Greenbaum SG, Suarez S, Kano K, Furukawa T (2004) J Phys Chem B 108:18832
33. Vittadello M, Suarez S, Fujimoto K, Noto VD, Greenbaum SG, Furukawa T (2005) J Electrochem Soc 152:A956
34. Suthanthiraraj SA, Premchand YD (2003) Ionics 9:301
35. Suthanthiraraj SA, Sheeba DJ, Paul BJ (2009) Mater Res Bull 44:1534
36. Ferry A, Jacobsson P, Stevens JR (1996) J Phys Chem 100:12574
37. Albinsson I, Mellander BE, Stevens JR (1992) J Chem Phys 96:681
38. Noto VD, Longo D, Munchow V (1999) J Phys Chem B103:2636
39. Marcinek M, Bac A, Lipka P, Zalewska A, Zukowska G, Borkowska R, Wieczorek W (2000) J Phys Chem B 104:11088
40. Wieczorek W, Florjanczyk Z, Stevens JR (1995) Electrochim Acta 40:2251
41. Jonscher AK (1981) J Mater Sci 16:2037
42. Cramer C, Funke K, Seatkamp T, Wilmer D, Ingram MD (1995) Z Naturforsch 50a:613
43. Gogulamurali N, Suthanthiraraj SA, Maruthamuthu P (1996) Solid State Ionics 86–88:1403
44. Hodge IM, Ingram MD, West AR (1976) J Electroanal Chem 74:125